Philosophical Magazine
Publication details, including instructions for authors and subscription information:
http://www.tandfonline.com/loi/tphm20

A numerical study of the overlap probability distribution and its sample-to-sample fluctuations in a mean-field model

Giorgio Parisi [a] & Federico Ricci-Tersenghi [a]
[a] Dipartimento di Fisica, INFN - Sezione di Roma 1 and CNR - IPCF, UOS di Roma, Università La Sapienza, P.le A. Moro 5, 00185 Roma, Italy
Version of record first published: 02 Dec 2011.

To cite this article: Giorgio Parisi & Federico Ricci-Tersenghi (2012): A numerical study of the overlap probability distribution and its sample-to-sample fluctuations in a mean-field model, Philosophical Magazine, 92:1-3, 341-352

To link to this article: http://dx.doi.org/10.1080/14786435.2011.634843

Philosophical Magazine
Vol. 92, Nos. 1–3, 1–21 January 2012, 341–352

Taylor & Francis
Taylor & Francis Group

A numerical study of the overlap probability distribution and its sample-to-sample fluctuations in a mean-field model

Giorgio Parisi* and Federico Ricci-Tersenghi

Dipartimento di Fisica, INFN – Sezione di Roma 1 and CNR – IPCF, UOS di Roma, Università La Sapienza, P.le A. Moro 5, 00185 Roma, Italy

(*Received 2 August 2011; final version received 28 September 2011*)

In this paper we study the fluctuations of the probability distributions of the overlap in mean-field spin glasses in the presence of a magnetic field on the De Almeida–Thouless line. We find that there is a large tail in the left part of the distribution that is dominated by the contributions of rare samples. Different techniques are used to examine the data and to stress different aspects of the contribution of rare samples.

Keywords: disordered systems; statistical mechanics; magnetism

1. Introduction

Spin glass models show amazing physical properties. Let us consider for simplicity mean-field spin glasses, like the Sherrington–Kirkpatrick model [1], whose solution is given by the hierarchical replica symmetry breaking (RSB) Ansatz [2–7]. The model is defined by the following Hamiltonian

$$\mathcal{H}[\vec{\sigma}] = -\sum_{i,j} J_{ij}\sigma_i\sigma_j, \tag{1}$$

where $\sigma_i = \pm 1$ are N Ising spins and the J_{ij} are quenched random couplings with zero mean and variance $1/N$.

For each sample $\mathcal{J}$, that is for a choice of the quenched random couplings, one can compute the probability distribution function of the overlap, $q = \sum_{i=1}^{N} \sigma_i\tau_i/N$, between two replicas $\vec{\sigma}$ and $\vec{\tau}$ subject to the same Hamiltonian (1): we call $P_{\mathcal{J}}(q)$ such a probability distribution.

In the Sherrington–Kirkpatrick model the order parameter in the thermodynamic limit is given by a function $q(x)$: $[0, 1] \to [0, 1]$, related to the probability distribution $P(q)$ of finding two replicas at an overlap q, where $P(q)$ is defined as

$$P(q) = \overline{P_{\mathcal{J}}(q)},$$

and the overline represents the average over the samples, $\mathcal{J}$.

*Corresponding author. Email: giorgio.parisi@roma1.infn.it

ISSN 1478–6435 print/ISSN 1478–6443 online

http://dx.doi.org/10.1080/14786435.2011.634843
http://www.tandfonline.com

The overlap distribution $P_{\mathcal{J}}(q)$ strongly fluctuates from sample to sample. In the low-temperature spin glass phase ($T < T_c$), these distributions are not self-averaging, that is the typical $P_{\mathcal{J}}(q)$ is very different from the disorder averaged distribution $P(q)$, even in the thermodynamic limit. The size of these fluctuations in the Sherrington–Kirkpatrick model can be quantified by using the Ghirlanda–Guerra relations [3,8–11]; the simplest identity is

$$\overline{P_{\mathcal{J}}(q)P_{\mathcal{J}}(q')} - \overline{P_{\mathcal{J}}(q)}\,\overline{P_{\mathcal{J}}(q')} = \frac{1}{3}\Big[\delta(q-q') - P(q)\Big]P(q'),$$

and the right-hand side is non-null as long as the $P(q)$ is not a delta function, i.e. when replica symmetry is broken.

These large sample-to-sample fluctuations play a very relevant role in numerical simulations, since they require a huge number of samples to obtain reliable measurements in the low-temperature phase of spin glass models, and they may produce finite size effects that vanish very slowly with increasing system size.

In the present paper we study overlap distributions in a mean-field spin glass model, defined on a Bethe lattice of fixed degree, in the presence of an external field. We focus on the data measured at the critical temperature T_c, such that the mean overlap distribution in the thermodynamic limit is a delta function, $P(q) = \delta(q - q_0)$. This choice has two main advantages:

- we know analytically the value of T_c and q_0, by solving the model with the cavity method, and this allows us to better study deviations from the thermodynamic limit (i.e. finite size effects);
- the system is critical and so it shows very large sample-to-sample fluctuations.

For any temperature different from T_c one of the above two statement would be false, thus making our study less interesting. Moreover the presence of the external field breaks the global spin inversion symmetry and implies that overlaps are non-negative in the thermodynamic limit: however it is well known that a large tail in the negative overlap region is present in systems of finite size and its origin needs to be clarified.

2. The model and the numerical simulations

We study an Ising spin glass model defined on a Bethe lattice of fixed connectivity $c = 4$ (i.e. a random regular graph of fixed degree $c = 4$). The Hamiltonian is

$$\mathcal{H} = -\sum_{\langle ij \rangle} J_{ij}\sigma_i\sigma_j - H\sum_i \sigma_i, \tag{2}$$

where $\sigma_i = \pm 1$ are N Ising spins, the couplings $J_{ij} = \pm 1$ (with equal probability) are quenched random variables and the sum runs over all pairs of neighboring vertices in the graph. We use a constant external field $H > 0$. For not very small connectivity, Ising spin glasses on a Bethe lattice share many properties with the Sherrrington–Kirkpatrick model [12,13]: in the limit $c \to \infty$ we recover the Sherrington–Kirkpatrick model, and the $1/c$ corrections are well under control [14].

We construct the random regular graph in the following way: we attach c legs to each vertex and then we recursively join a pair of legs, forming a link, until no legs are left or a dead end is reached (this may happen because we avoid self-linking of a vertex and double-linking between the same pair of vertices); if a dead end is reached, the whole construction is started from scratch.

Similarly to the Sherrrington–Kirkpatrick model, the model (2) has a continuous spin glass phase transition at a critical temperature T_c which depends both on the value of c and H. At variance with the Sherrrington–Kirkpatrick model, the critical line in the (T, H) plane does not diverge when $T \to 0$, but rather reaches a finite value H_c (see Figure 1). This is due to the finite number of neighbors each spin has on a random graph of finite mean degree (while this number is divergent with the system size in the Sherrrington–Kirkpatrick model). In this sense the present model is closer to finite dimensional models than the Sherrrington–Kirkpatrick model is.

The replica symmetric (RS) phase of model (2) can be solved analytically by the cavity method [13]. In particular one can find the boundary of the RS phase, beyond which the model solution spontaneously breaks the replica symmetry [15,16]. In Figure 1 we show such a critical line in the (T, H) plane for the model with fixed degree $c = 4$. The high-temperature and/or high-field region is replica symmetric, while a breaking of the replica symmetry is required in the low-temperature and low-field region. We have checked that the phase boundary behaves like $H_c(T) \propto (T - T_c)^{3/2}$ close to the zero-field critical point T_c, and the exponent is the same as that found in the Sherrrington–Kirkpatrick model.

We have carried our Monte Carlo simulations at the point marked with the big dot in Figure 1, that is $H = 0.7$ and $T = 0.73536$. The uncertainty in the critical temperature for $H = 0.7$ is 10^{-5}. At that point the value of the thermodynamic overlap is $q_0 = 0.67658(1)$. Please note that we have chosen a rather large value of the

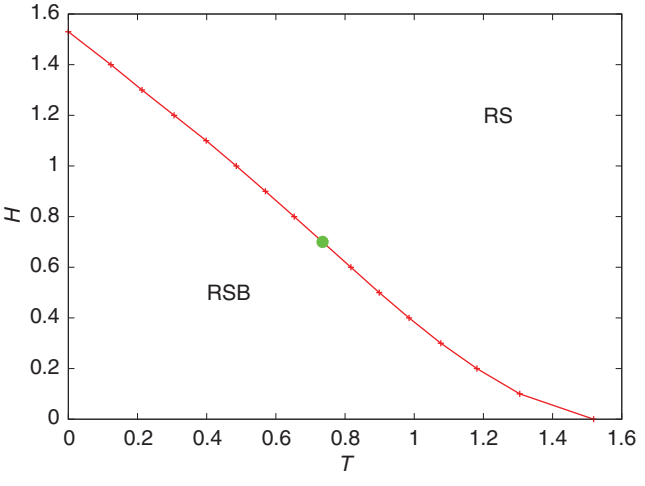

Figure 1. (Color online). Phase diagram in the temperature–field plane for the $J = \pm 1$ spin glass model defined on a Bethe lattice of fixed degree $c = 4$. In this work we report data collected at the critical point marked by the big dot.

external field, which is roughly half of the largest critical field value $H_c(T=0) \simeq 1.53$, in order to avoid crossover effects that could be due to the vicinity of the zero-field critical point.

Monte Carlo simulations have been performed by using the Metropolis algorithm and the parallel tempering method: we used 20 temperatures equally spaced between $T_{\max} = 2.0$ and $T_c = 0.73536$, and we attempted the swap of configurations at nearest temperatures every 30 Monte Carlo sweeps (MCS). Each sample (of any size) has been thermalized for 2^{24} MCS and then 1024 measurements have been taken during another 2^{26} MCS: so there are 2^{16} MCS between two successive measurements and we have checked this number to be larger than the autocorrelation time. We study systems of sizes ranging from $N = 2^6$ to $N = 2^{14}$, with the number of samples ranging from 5120 for $N = 2^6$ to 1280 for $N = 2^{14}$. We are going to present only the data for sizes $N \leq 2^{12}$ for which we have simulated at least 2560 samples; indeed the data for $N = 2^{13}$ and $N = 2^{14}$ are more noisy (due to the limited number of samples); moreover we fear that some samples may not be perfectly thermalized even after 2^{26} MCS. By restricting to $N \leq 2^{12}$ we are fully confident about the numerical data.

3. Results

We start by showing in Figure 2 the disorder averaged $P(q)$ for different sizes. The exponential tail on the left side is evident from the plot (which is on a logarithmic scale): this tail goes far into the negative overlap region for small sizes. In the following we are going to show that this exponential tail is not a feature of typical samples, but it is completely due to very rare and atypical samples.

The vertical line at $q = q_0$ in Figure 2 marks the location of the delta peak in the thermodynamic limit. By looking at the mean and the variance of $P(q)$ we have checked how finite size effects decay to zero. We see in Figure 3 that while $\overline{\langle q^2 \rangle}_c$

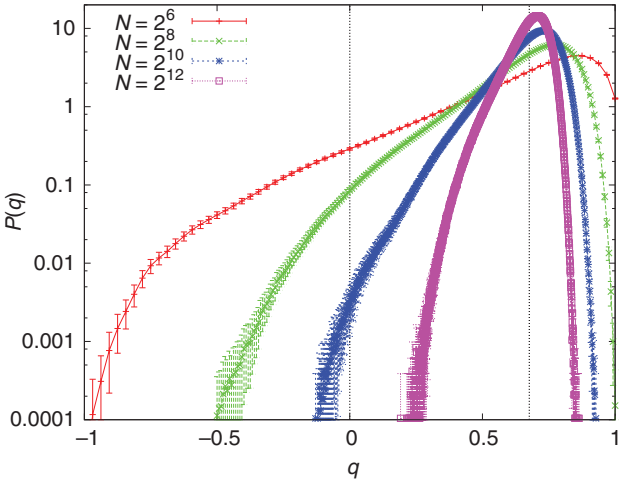

Figure 2. (Color online). Disorder averaged overlap probability distributions $P(q)$ show an exponential tail for $q < q_0$.

decays in a way compatible with the expected behavior $N^{-2/3}$ (the discrepancy can be well explained in terms of small scaling corrections), the mean overlap $\overline{\langle q \rangle}$ shows finite size corrections proportional to $N^{-1/2}$ (instead of the expected $N^{-1/3}$) and seems to extrapolate to a thermodynamic limit different from q_0. This means that a naive extrapolation to the thermodynamic limit would produce an incorrect estimate of q_0. The most probable explanation is that finite size corrections of order $N^{-1/2}$ have a much larger coefficient than those of order $N^{-1/3}$ and then much larger sizes are needed to observe the asymptotic behavior.

A much better way to estimate q_0 from the disorder averaged data seems to be the analysis of the overlap integrated probability function

$$x(q) \equiv \int_{-1}^{q} P(q')\mathrm{d}q'.$$

This variable has been used for studying the behavior of three-dimensional systems at zero magnetic field [17,18]. The results are shown in Figure 4. In the main panel we

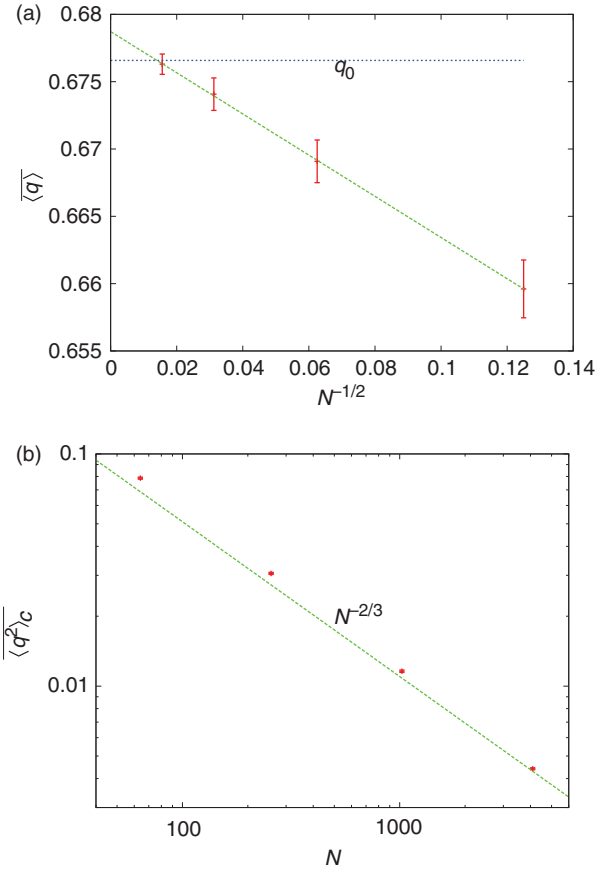

Figure 3. (Color online). Mean (a) and variance (b) of $P(q)$. A naive analysis would predict an asymptotic value for $\langle q \rangle$ larger than q_0 and finite size corrections decaying faster than the $N^{-1/3}$ expected behavior. The variance decays roughly as the expected $N^{-2/3}$ law.

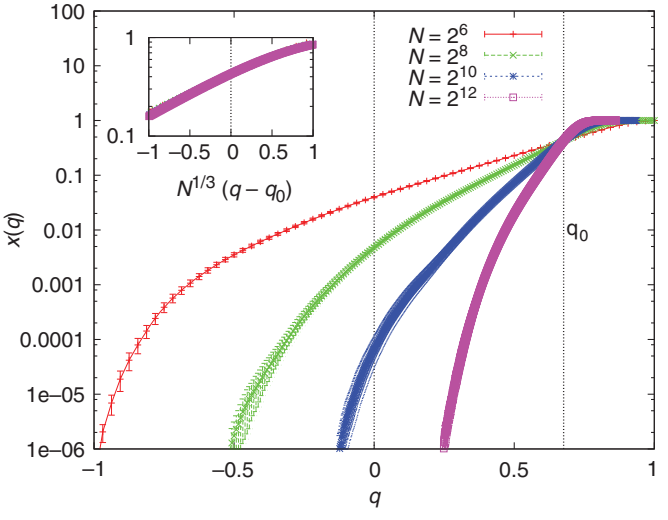

Figure 4. (Color online). The integrated probability distribution $x(q)$ averaged over the disorder. The value of q_0 can be well determined by the crossing point of the data set in the main panel. The inset show the scaling function $x(N^{1/3}(q-q_0))$.

see again the exponential tail on the left side, but the crossing point of the functions $x(q)$ estimates with a high accuracy the right value for q_0. In the present case all the crossing points for the sizes shown are within a distance less than 10^{-3} from the thermodynamic value and converge to it according to an $N^{-1/3}$ law. In the inset of Figure 4 we show that $x(q)$ data perfectly collapse when plotted as a function of the scaling variable $N^{1/3}(q-q_0)$. On the contrary, we have found that by plotting $P(q)/N^{1/3}$ versus $N^{1/3}(q-q_0)$ the scaling is very poor (data not shown), thus suggesting the presence of a very strong correction to scaling.

Let us now turn to the study of sample-to-sample fluctuations. We want to convince the reader that the exponential tail is not a feature of typical samples: actually not even a feature of the vast majority of samples, which show roughly Gaussian (or even steeper) tails in their $P_{\mathcal{J}}(q)$. The exponential tail is produced by the integration of the secondary peak that atypical samples have at an overlap value much smaller than q_0.

Extracting typical and atypical shapes of the $P_{\mathcal{J}}(q)$ from thousands of samples is not a straightforward job. We follow the simplest procedure based on the analysis of the first two moments. In the main panel of Figure 5 we show the mean and the variance of the 2560 samples of size 2^{12}. The three insets in Figure 5 show the averages over 20 $P_{\mathcal{J}}(q)$ chosen from typical samples (lower inset) or from atypical samples, either much broader or much narrower than typical (upper insets). In every inset we also draw a dashed vertical line to mark the location of q_0.

We notice that there exists a large difference between typical and atypical samples, both quantitatively and qualitatively (especially for the atypical samples showing a double peak structure). However the very different shapes can be roughly accounted for by considering an effective external field different from the one ($H = 0.7$ in the present case) appearing in the Hamiltonian: in the atypical samples

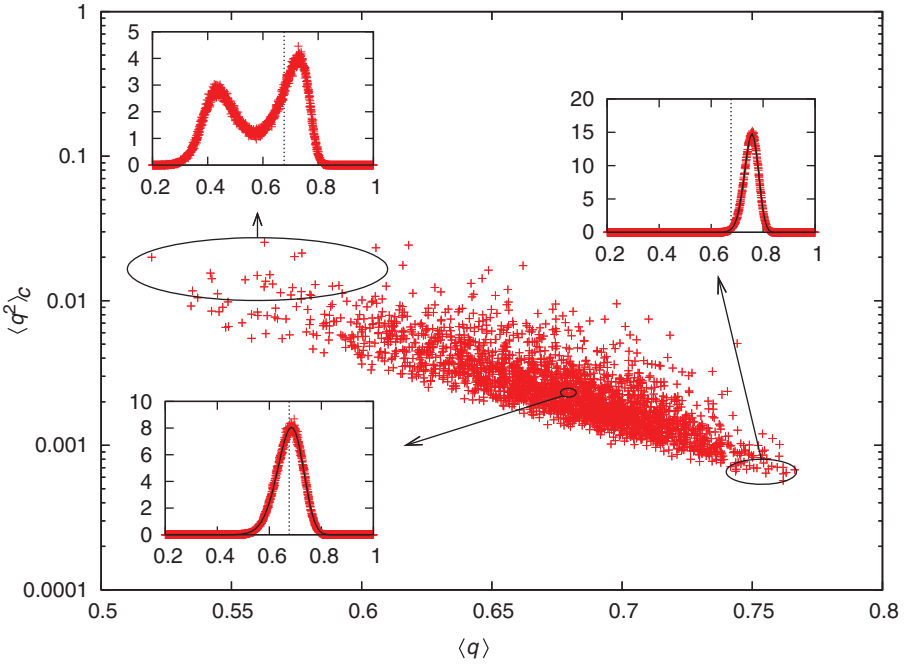

Figure 5. (Color online). Mean and variance of the 2560 samples of size $N = 2^{12}$. Insets show the overlap probability distribution averaged over a small fraction, 1/128, of samples (those in the corresponding circle). Solid curves in the insets are Gaussian fits to the data (see text for details).

shown in the upper right inset this effective field is larger than H and thus the overlap distribution is narrower and centered on a value greater than q_0, while the atypical samples shown in the upper left inset look as if they were below the critical line, i.e. with a field smaller than H.

Since samples with different effective fields will have different critical temperatures, it is possible that the main source of sample-to-sample fluctuations can be well described by a random temperature (or field) term in the effective Hamiltonian as in the case of ferromagnets in a random magnetic field [19–21].

It is also worth noticing that the tails of the distributions shown in the insets of Figure 5 are Gaussian or even steeper, as expected [22,23]. Indeed, the interpolating curves superimposed to the bimodal distributions (lower left and upper right insets) have been obtained by assuming $q = \tanh(h)$ with a Gaussian distributed local field h. The nonlinear transformation is necessary (and sufficient) to take into account the small skewness of the distributions.

In Figure 5 we have presented data only for size $N = 2^{12}$, but a natural question is how sample-to-sample fluctuations vary with the system size. We have found that by increasing the system size the distribution of the moments shrinks towards the thermodynamic limits ($\langle q \rangle = q_0$ and $\langle q^2 \rangle_c = 0$) with the expected $N^{-1/3}$ scaling behavior. However it is not true that all samples become typical in the thermodynamic limit. In other words, the fraction of atypical samples (e.g. those with a bimodal distribution) remains roughly constant. In Figure 6 we show the average

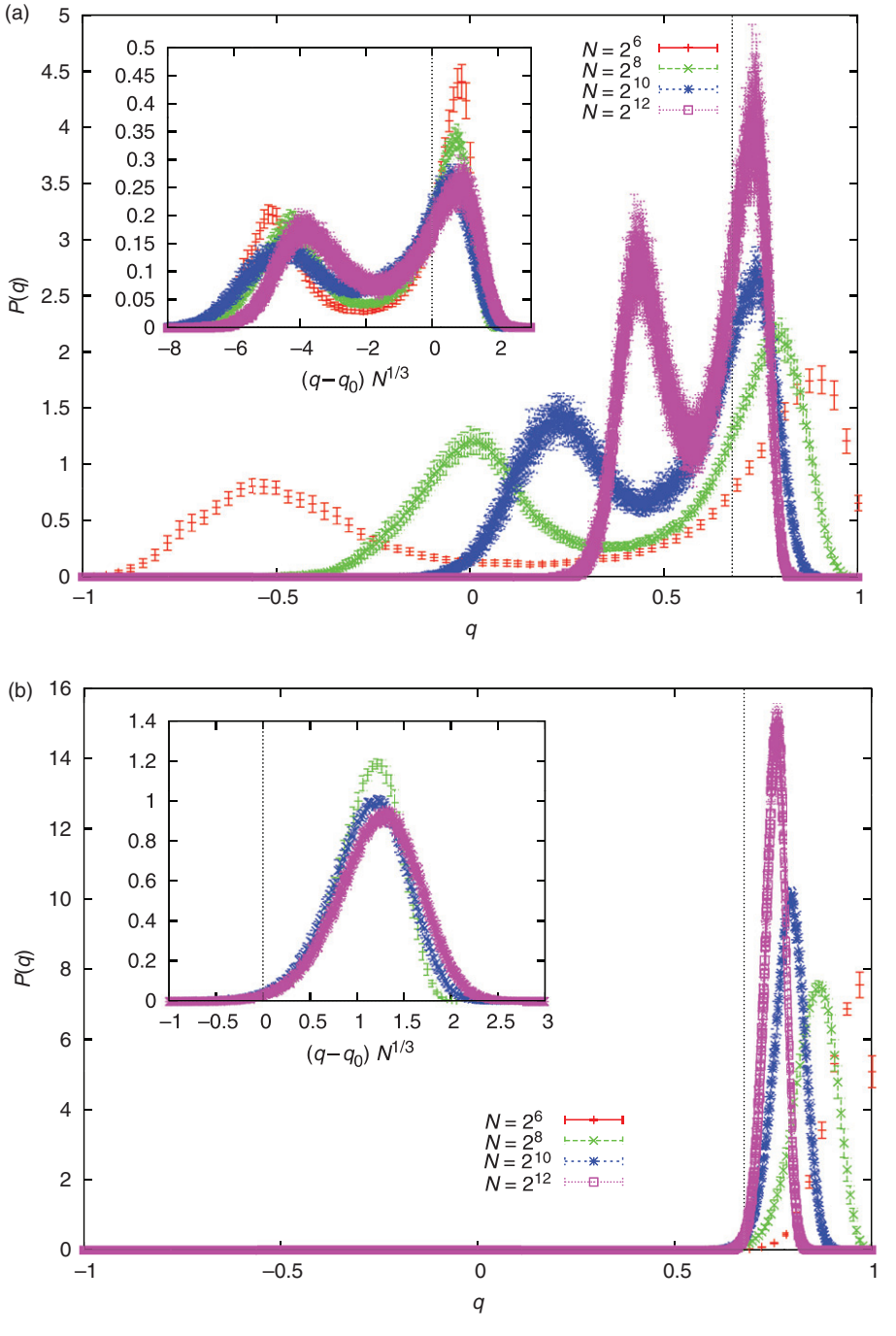

Figure 6. (Color online). Most atypical distributions, averaged over a fraction 1/128 of samples: those with the largest (a) and smallest (b) variance. By varying the system size they roughly preserve the shape and get shrunk according to the scaling $q - q_0 \sim N^{-1/3}$ (see insets).

$P(q)$ computed on a small fraction (1/128) of samples, those most atypical, i.e. those corresponding to upper insets in Figure 5. We notice that, by varying the size, the shape is more or less preserved and the main effect is an overall shrink of the distribution. The insets in Figure 6 show that this shrinking is consistent with the scaling law $q - q_0 \sim O(N^{-1/3})$ which holds at criticality.

Given that neither typical nor atypical distributions have an exponential tail, the only possible explanation is that such a tail is generated by the secondary peak of broader distributions when averaging over the samples. We are going to provide quantitative evidence for this by looking at the integrated probabilities

$$X_{\mathcal{J}}(q) \equiv \int_{-1}^{q} P_{\mathcal{J}}(q')\mathrm{d}q'.$$

Let us define the moments of the random variable $X_{\mathcal{J}}$ as

$$X_k(q) \equiv \overline{X_{\mathcal{J}}(q)^k}.$$

Recall that $X_1(q) = x(q)$ is plotted in Figure 4 and shows an exponential tail. However in the region $q \ll q_0$ the average $X_1(q)$ is dominated by rare samples, while the vast majority of samples have a very small value $X_{\mathcal{J}}(q) \ll X_1(q)$ and do not contribute to $X_1(q)$.

In order to extract the behavior of typical samples one should average the random variable $\log(X_{\mathcal{J}}(q))$. However for $q \ll q_0$ there are samples with $X_{\mathcal{J}}(q) = 0$ and a straightforward computation of $\overline{\log[X_{\mathcal{J}}(q)]}$ is not possible. However, by noticing that

$$\overline{\log[X_{\mathcal{J}}(q)]} = \lim_{k \to 0} \log\left[X_k(q)^{1/k}\right],$$

it is possible to observe the behavior of typical samples by choosing $0 < k \ll 1$. In Figure 7(a) we plot $X_k(q)$ for $k = 1, 1/4, 1/16, 1/64$ and we clearly see how the exponential tail for $k = 1$ becomes a Gaussian (or even steeper) decay for $k \ll 1$. Moreover this behavior is very well conserved by varying the system size: in Figure 7(b) we plot the same averages, X_1 to $X_{1/64}$, as a function of the scaling variables $N^{1/3}(q - q_0)$ and we see that the data collapse (which is very good for $q \simeq q_0$) remains a reasonable approximation in the entire q range. This observation suggests that the entire distribution of the random variable $X_{\mathcal{J}}(q)$ mainly depends on the scaling variable $N^{1/3}(q - q_0)$, or equivalently on the first moment X_1. This can be checked in Figure 8 where we plot the distribution of $X_{\mathcal{J}}$ at some fixed value of X_1 for several system sizes. Please note that the data for $X_1 = 1/64$ have been multiplied by a factor of 10 in order to avoid overlaps with other data sets and improve readability.

From Figure 8 we can finally draw the main conclusions of this analysis. First of all, the good data collapse for the probability distribution of $X_{\mathcal{J}}$ at a fixed value of X_1 is a strong indication that we have measured large enough systems in the asymptotic scaling regime. Moreover we see that for $X_1 = 1/2 > x(q_0) \simeq 0.429$ the distribution of $X_{\mathcal{J}}$ has a maximum close to X_1, that is the mean value is representative of typical sample behavior. On the contrary, for $X_1 < x(q_0)$, the distributions of $X_{\mathcal{J}}$ have their maxima at $X_{\mathcal{J}} \simeq 0$ and the mean value is not

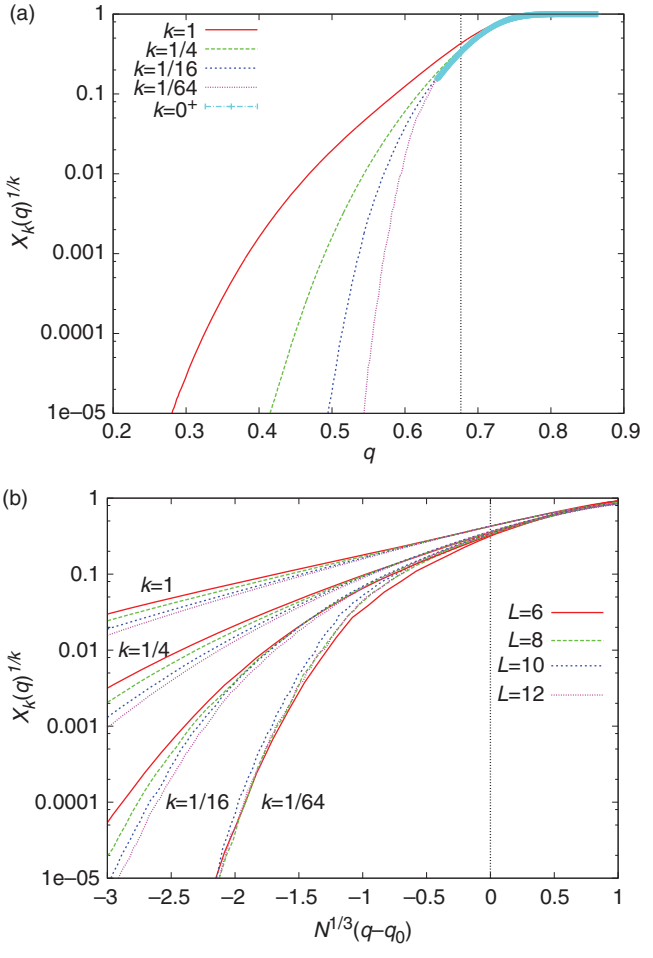

Figure 7. (Color online). (a) Small k moments of $X_{\mathcal{J}}(q)$ measured in systems of size $N = 2^{12}$ show a decay faster than exponential for $q \ll q_0$. (b) Systems of different sizes show the same behavior, once the overlap is rescaled accordingly.

representative of typical values. In particular we observe that for very small values of X_1 the distribution of $X_{\mathcal{J}}$ develops a power-law divergence $1/X_{\mathcal{J}}$ for $X_{\mathcal{J}} \to 0$.

4. Conclusions

In this paper we have seen that on the De Almeida–Thouless line the left tail of the distribution of $P(q)$ is dominated by rare samples. The presence of a left tail in the probability is quite an annoying phenomenon that is present also in the Sherrington–Kirpatrick model [24,25] and in finite dimensional models [26], both at the phase transition point and below the transition. This tail is particularly bothersome at not too large magnetic field, because it extends into the region of negative q. We think

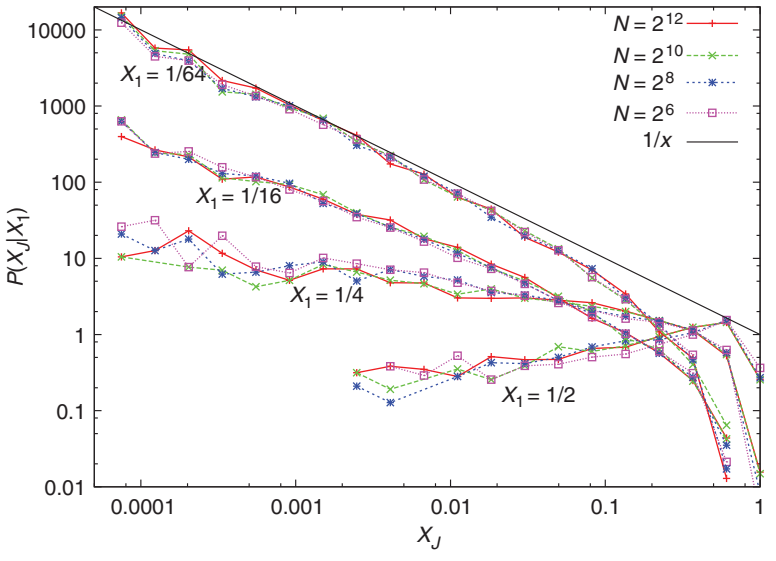

Figure 8. (Color online). Histograms of $X_{\mathcal{J}}$ at fixed values of X_1. The data for $X_1 = 1/64$ has been multiplied by 10 in order to improve readability.

that understanding the origin of this tail may be useful in future analysis of the finite dimensional simulations.

It would be very useful to derive the results in this paper in an analytical way extending the techniques of [22]. Indeed in that paper the computation of the tail was done for the typical samples and we have to modify it in order to compute the tail of the average over the samples. We believe that this is a feasible task.

References

[1] D. Sherrington and S. Kirkpatrick, Phys. Rev. Lett. 35 (1975) p.1792.
[2] E. Marinari, G. Parisi, F. Ricci-Tersenghi, J. Ruiz-Lorenzo and F. Zuliani, J. Stat. Phys. 98 (2000) p.973.
[3] M. Mézard, G. Parisi and M.A. Virasoro, *Spin Glass Theory and Beyond*, World Scientific, Singapore, 1987.
[4] G. Parisi, *Field Theory, Disorder and Simulations*, World Scientific, Singapore, 1992.
[5] F. Guerra, Comm. Math. Phys. 233 (2003) p.1.
[6] M. Talagrand, C. R. Acad. Sci. Paris, Ser. I 337 (2003) p.111.
[7] M. Talagrand, Ann. Math. 163 (2006) p.221.
[8] D. Ruelle, Comm. Math. Phys. 48 (1988) p.351.
[9] S. Ghirlanda and F. Guerra, J. Phys. A: Math. Gen. 31 (1998) p.9149.
[10] M. Aizenman and P. Contucci, J. Stat. Phys. 92 (1998) p.765.
[11] G. Parisi, Int. J. Mod. Phys. B 18 (2004) p.733.
[12] L. Viana and A.J. Bray, J. Phys. C 18 (1985) p.3037.
[13] M. Mézard and G. Parisi, Eur. Phys. J. B 20 (2001) p.217.
[14] G. Parisi and F. Tria, Eur. Phys. J. B 30 (2002) p.533.

[15] A. Pagnani, G. Parisi and M. Ratiéville, Phys. Rev. E 68 (2003) p.046706.
[16] H. Takahashi, F. Ricci-Tersenghi and Y. Kabashima, Phys. Rev. B 81 (2010) p.174407.
[17] E. Marinari, G. Parisi and J.J. Ruiz-Lorenzo, Phys. Rev. B 58 (1998) p.14852.
[18] R. Alvarez Baños, A. Cruz, L.A. Fernandez, J.M. Gil-Narvion, A. Gordillo-Guerrero, M. Guidetti, D. Iñiguez, A. Maiorano, F. Mantovani, E. Marinari, V. Martin-Mayor, J. Monforte-Garcia, A. Muñoz-Sudupe, D. Navarro, G. Parisi, S. Perez-Gaviro, F. Ricci-Tersenghi, J.J. Ruiz-Lorenzo, S.F. Schifano, B. Seoane, A. Tarancon, R. Tripiccione and D. Yllanes, Phys. Rev. B (in press).
[19] N. Sourlas, Comput. Phys. Commun. 121–122 (1999) p.183.
[20] G. Parisi and N. Sourlas, Phys. Rev. Lett. 89 (2002) p.257204.
[21] G. Parisi, M. Picco and N. Sourlas, Europhys. Lett. 66 (2004) p.465.
[22] S. Franz, G. Parisi and M. Virasoro, J. Phys. I France 2 (1992) p.1869.
[23] A. Billoire, S. Franz and E. Marinari, J. Phys. A 36 (2003) p.15.
[24] A. Billoire and B. Coluzzi, Phys. Rev. E 67 (2003) p.036108.
[25] A. Billoire and B. Coluzzi, Phys. Rev. E 68 (2003) p.026131.
[26] L. Leuzzi, G. Parisi, F. Ricci-Tersenghi and J.J. Ruiz-Lorenzo, Phys. Rev. Lett. 103 (2009) p.267201.